ChemEngineering

MDPI

Article

Using Differential Scanning Calorimetry to Measure the Energetic Properties of Residual Sludge and Catalysts from the Textile, Tannery, and Galvanic Industries

Ghem Carvajal-Chávez, Josselyn Cazar, Gilda Gordillo, Andrés De-La-Rosa, Gonzalo Chiriboga and Carolina Montero-Calderón *

Facultad de Ingeniería Química, Universidad Central del Ecuador, Ritter s/n & Bolivia, Quito 170402, Ecuador; gcarvajal@uce.edu.ec (G.C.-C.); josselyn.cazar@gmail.com (J.C.); gggordillo@uce.edu.ec (G.G.); adelarosa@uce.edu.ec (A.D.-L.-R.); wgchiriboga@uce.edu.ec (G.C.)
* Correspondence: cdmontero@uce.edu.ec

Abstract: This research delved into the energetic properties of catalysts synthesized from residual sludge from the textile, galvanic, and tannery industries. The experimental process consisted of an initial heat treatment to activate their catalytic properties and a thermal analysis employing differential scanning calorimetry (DSC). This technique permitted the investigation of the materials' thermal behavior as a function of temperature, ranging from 142 to 550 °C, effectively controlling the heating rates and pressure conditions. The data gathered were the input for constructing specific heat models through polynomial regression employing the least squares method. These models were subsequently used to estimate variations in the enthalpy and entropy for both the sludge and catalysts through integration. Third-degree polynomials primarily characterized the specific heat models that accurately represented the samples' thermal behavior, considering variations in their physicochemical properties that influenced it. The catalysts derived from residual sludge from the textile industry exhibited the models with the most robust statistical fit. Concurrently, the catalysts from the galvanic industry displayed noteworthy similarities with the bibliographic data across various temperature points. The mathematical models determined the specific heat (Cp) as a function of temperature, which, in turn, was used to estimate the enthalpy and entropy variations in the sludge and catalysts under study. The highest enthalpy value corresponded to the sludge and catalyst obtained from the tannery industry, with a Cp of 5.60 J/g-K at 603 K and 2.45 J/g-K at 445.6 K. Finally, the third-degree polynomials showed the best mathematical models since (1) they considered the variations in the physicochemical properties that intervened in the behavior of Cp as a function of temperature; (2) they presented a better statistical fit; and (3) they showed consistency with the existing information in the literature for the textile industry and the galvanic industries.

Keywords: catalyst; sewage sludge; differential scanning calorimetry; specific heat; enthalpy; entropy

Citation: Carvajal-Chávez, G.; Cazar, J.; Gordillo, G.; De-La-Rosa, A.; Chiriboga, G.; Montero-Calderón, C. Using Differential Scanning Calorimetry to Measure the Energetic Properties of Residual Sludge and Catalysts from the Textile, Tannery, and Galvanic Industries. *ChemEngineering* **2024**, *8*, 123. https://doi.org/10.3390/chemengineering8060123

Academic Editor: Maria del Carmen Marquez

Received: 12 August 2024
Revised: 13 October 2024
Accepted: 1 November 2024
Published: 3 December 2024

1. Introduction

In 2022, Ecuador enacted a law fostering the circular economy [1] to promote the trade of waste materials, especially from the manufacturing industries. In this context, previous research conducted by this group has synthesized catalysts from sewage sludge from the textile, galvanic, and tannery industries, as well as from petroleum storage tank bottoms and mining tailings. These catalysts, primarily composed of iron, have demonstrated activity, particularly for petroleum cracking reactions and catalytic methane decomposition. The highest specific surface area for catalysis was 31.73 m^2/g [2] for waste sludge from the textile industry, followed by 20.05 m^2/g for the tannery industry [3] and 17.68 m^2/g [3] for the galvanic industry. Studying the thermodynamic properties of these materials could be a valuable tool for exploring reuse options to produce high-value-added products that contribute to the circular economy.

Thermal analysis is considered highly valuable for the synthesis and characterization of catalysts. Well-known techniques include thermal differential studies and differential scanning calorimetry (DSC), with heat flows applied to metals and alloys to analyze these materials. These methods can determine the potential of the reuse of catalysts while minimizing the activity loss [4] and can be used to analyze metallic transitions.

Furthermore, DSC has enabled the development of kinetic models for reactions involving metallic catalysts, such as the combustion of petroleum with metallic chlorides [5] and the catalytic combustion of methane over cobalt catalysts [6].

DSC has also been used to evaluate the hazard characteristics of metallic nanopowders, assessing the explosion potential of materials derived from iron and zinc [7]. Determining the thermal properties of a catalyst (its specific heat, enthalpy, and entropy) is essential for defining the operational conditions in real reactors. The heat capacity of a catalyst can significantly influence a reactor's temperature and heat flux, thus impacting the energy balance significantly. Safety risks encompass mechanical issues (such as reactor overpressurization), chemical concerns (including corrosion and the initiation of alternative reactions), and physical hazards (such as burns resulting from the release of vapors and thermal stress). These aspects are essential for robust modeling and simulation, constituting the basis of reliable chemical process design and operation.

Nevertheless, there is still a need for more comprehensive information regarding the performance of sludge and metals used as catalysts. High surface temperatures promote reaction development for catalytic materials. Consequently, the heat transfer phenomenon and temperature profiles under wet or dry conditions influence the catalytic activity. There is a growing interest in studying the energetic properties of catalytic materials and residual sludge from textile, tannery, and galvanic industries. These studies are linked to processes involving heat addition or extraction. The primary objective is to identify alternative options for the commercial catalysts currently employed in the industry by synthesizing catalysts from industrial residues. This interest in the energy valorization process also extends to the analysis of the original sludge.

Although some alternatives have been proposed for the valorization of this sewage [8], the present study employed DSC to ascertain the thermal variations in sludge and catalysts derived from industrial waste, yielding heat flux data across the 142 to 550 °C temperature range and developing specific heat models via polynomial regression using the least squares criterion, which satisfies the statistical criteria. These models were then employed to determine the enthalpy and entropy within various temperature intervals of integration. These findings can serve as a valuable tool for utilizing these materials in other chemical and industrial reaction processes, thereby enabling the scaling of catalyst production derived from the sludge due to its metallic content [9,10]. Some applications include the catalytic decomposition of methane [11], homogeneous reactions, such as obtaining lactic acid [12], and wastewater treatment as sustainable methods to eliminate hazardous pollutants, demonstrating effectiveness in the degradation of bisphenol in hydrogen production [13].

2. The Methodological Framework

2.1. Experimental Design

Sludges from galvanic [3], textile [2], and tannery processes [14] were obtained from specific factories located in Quito and Ambato, Ecuador. The residual sludges were dried in ASTM-D2216 in a drying oven (Nabertherm-TR60, Bahnhofstr, Lilienthal, Germany) for four hours to prepare the catalysts. The dried sludges were sieved between 150 and 180 μm using Tyler's Sieve series. The sludges and catalysts obtained are shown in Figure 1.

Figure 1. Sludge and catalysts studied.

The residual sludges were calcined between 400 and 900 °C for four hours in a muffle furnace (Thermo Scientific—Thermolyne, Waltham, MA, USA). This process removed the organic residues and oxidized the metallic phase of the sludges. After the thermal process, the residual sludges were considered catalytic material.

This study aims to analyze how different temperatures affect the mechanical strength and textural properties of the materials. We utilized various techniques to characterize the structure, including elemental analysis, FTIR (Fourier-transform infrared spectroscopy), nitrogen adsorption, X-ray diffraction, and programmed temperature reduction. Finally,

we used industrial application reactions, such as those involving glycerol [2], crude oil [15], and methane thermal decomposition [16] for the catalytic properties.

The specifications of the properties of the samples used are shown in Table 1, according to the type of industry: textile [2], tannery [14], and galvanic [3]. The surface characteristics were examined with N2 adsorption–desorption utilizing a surface area analyzer (Horiba-SA 9600, Minami-ku, Kyoto, Japan). This device measures the gas adsorption and desorption profiles using the flowing gas technique, while the surface area is determined via the single-point BET approach. In preparation for the analysis, 0.15 g of the sample was placed in a U-tube and degassed at 300 °C for two hours to purify the surface. The N2 adsorption–desorption procedure was subsequently performed using liquid N2 (Enox S.A., Quito, Pichincha, Ecuador).

Table 1. Properties of sludge and catalysts.

Industry		Properties					
		% Humidity	T. Calcination (°C)	Oxides	Metal (Phase Act.)	Specific Surface (m^2/g)	Pore Volume (cm^3/g)
Textile	L1	76.50	-	-	Fe	-	-
	C1	-	600	Fe_2O_3, Al_2O_3, SiO_2, Cr_2O_3, ZnO, Ni_2O_3, Co_3O_4.		30.36	0.0375
	L2	66.01	-	-	Cr, Zn	-	-
	C2	-	600	Fe_2O_3, Al_2O_3, SiO_2, Cr_2O_3, ZnO, Ni_2O_3 y Co_3O_4		31.73	0.0518
Tannery	L3	12.65	-	-	-	-	-
	C3	-	400	Cr_2O_3		25.829	0.0250
Galvanic	L4	58.00	-	-	Fe, Zn	-	-
	C4	-	400	FeO, Fe_2O_3, Fe_3O_4 y ZnO.		96.15	0.12
	L5	53.83	-	-		-	-
	C5	-	500	FeO, Fe_2O_3, Fe_3O_4, ZnO.		63.36	0.09
	L6	74.47	-	-	Fe	-	-
	C6	-	550	FeO, Fe_3O_4.		17.68	0.02

2.2. Laboratory Method

A calorimeter NETZSCH 3500 Sirius located in the Thermodynamic Lab from Facultad de Ingenieria Quimica, Universidad Central del Ecuador carried out the energetic characterization of the sludge and catalysts, applying the ASTM E1269-1 [17].

The analysis was conducted using alumina crucibles with a capacity of 150 µL, containing a sample mass of 10 mg. The experiment was performed under a nitrogen atmosphere at a flow rate of 30 mL/min, with a temperature ramp of 15 °C/min during both isothermal and dynamic processes (Figure 2). The temperature was raised to 100 °C to eliminate the organic phase and any ambient moisture from the catalyst. This means that the calorimetry measurements did not account for phase changes such as evaporation. Additionally, temperatures were kept below 600 °C to prevent any fusion effects. The calorimetry results provided heat flow data (Φ) for the sludge and catalysts, which allowed for the estimation of energetic properties such as specific heat, enthalpy, and entropy using mathematical models.

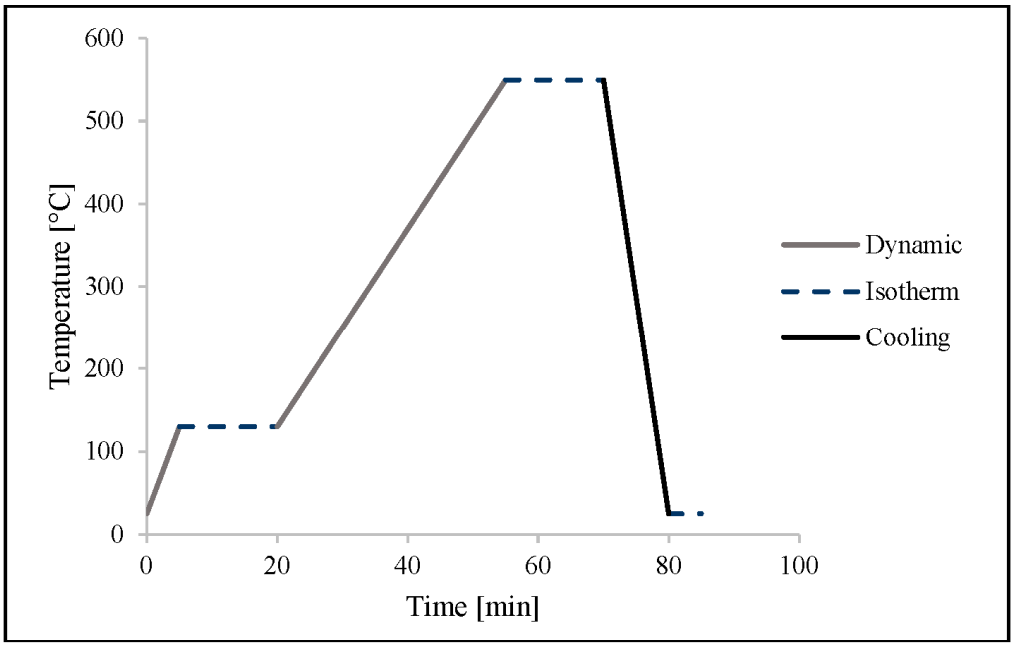

Figure 2. Methodology for the calorimetric analysis of sludge and catalysts.

2.3. Analysis of Data

The equation for specific heat allows us to determine its value as a function of temperature while defining important energy properties, including enthalpy and entropy. It also enables the description of various characteristics related to these properties. The way a material's specific heat varies is influenced by the temperature range being examined. Consequently, a preliminary analysis of the DSC thermogram is essential to identify the temperature intervals suitable for applying polynomial regression models.

The trend of the DSC thermograms and the high compatibility of the third-degree heat capacity with experimental data [18] sustain the selection of the following model:

$$Cp = a_1 + a_2T + a_3T^2 + a_4T^3 \quad (1)$$

The least squares method serves as a powerful technique for determining the partial slopes and intercepts of polynomial functions. By implementing variance analysis within our regression models, we can evaluate the statistical significance of our findings. Additionally, we appraise the model's efficacy through the adjusted coefficient of determination, which indicates the proportion of variability accounted for by the model. We also conducted thorough checks to ensure that our assumptions, including the normality and homogeneity of residual variances, are valid. Lastly, we quantified uncertainty by establishing confidence bands at an impressive 95% for our predicted values. This approach provides valuable insights into our analyses.

3. Results and Discussion

3.1. Differential Calorimetry Analysis

DSC thermograms are shown for each sample exposed to isothermal heating to 130 °C and dynamic heating from approximately 142 to 550 °C. In addition, note that the endothermic peaks in the thermograms are in the positive direction, as shown in Figure 3.

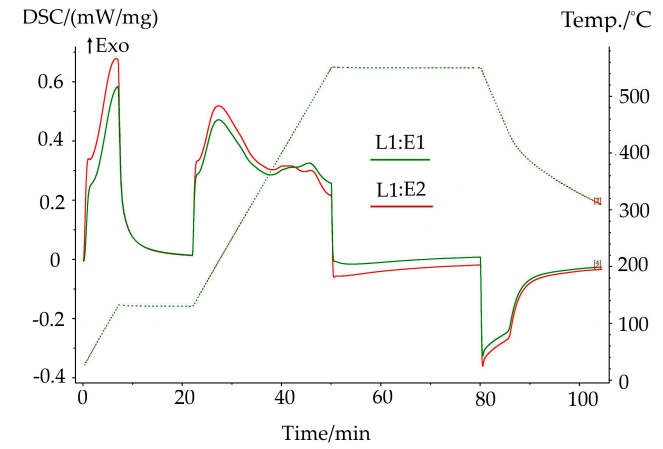

L1: Textile sludge 1

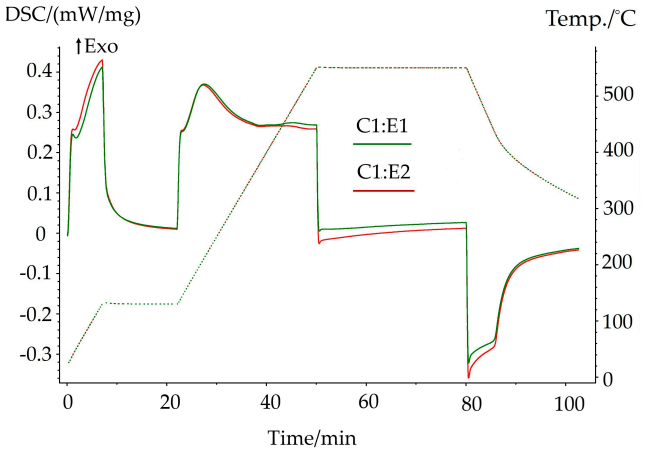

C1: Textile catalyst 1

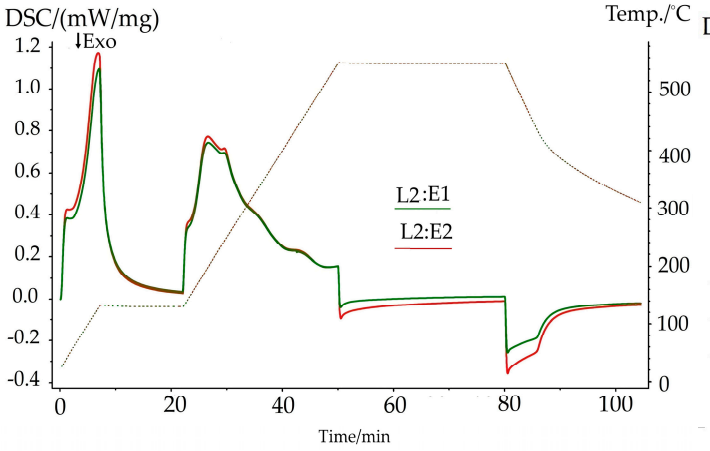

L2: Textile sludge 2

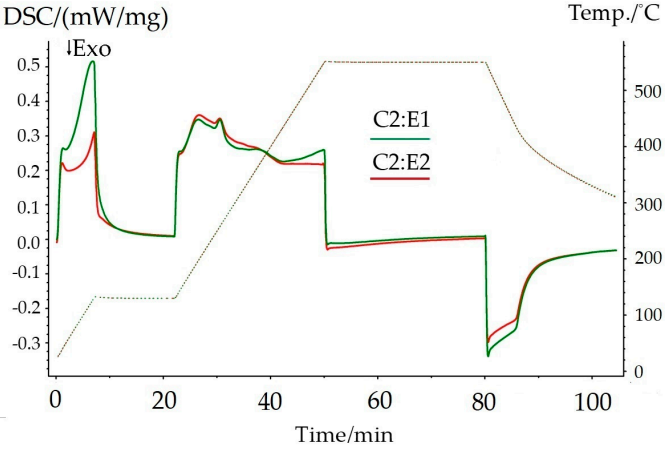

C2: Textile catalyst 2

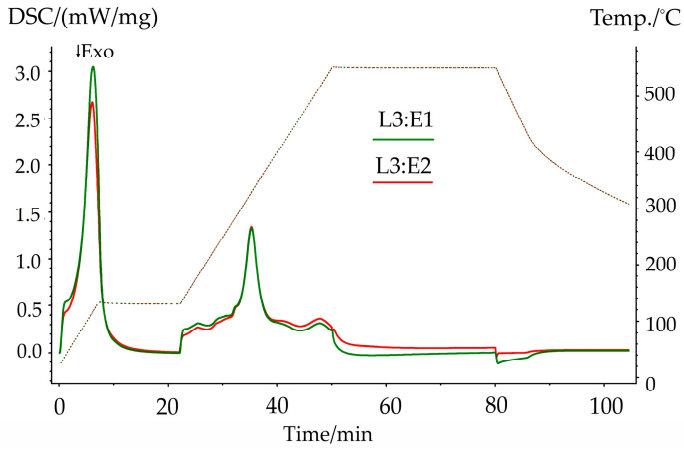

L3: Tannery sludge

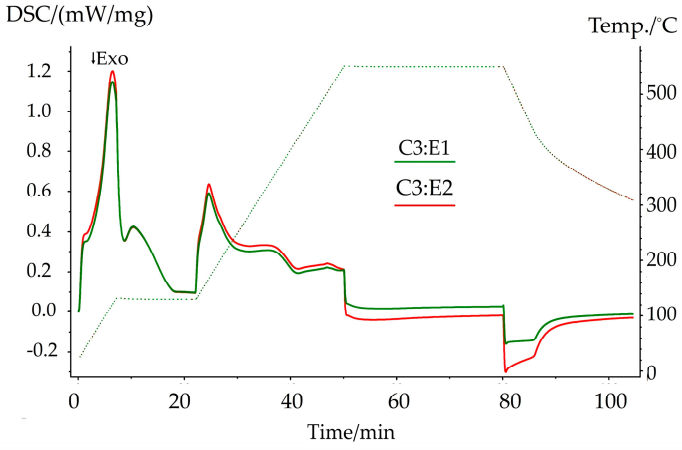

C3: Tannery catalyst

Figure 3. *Cont.*

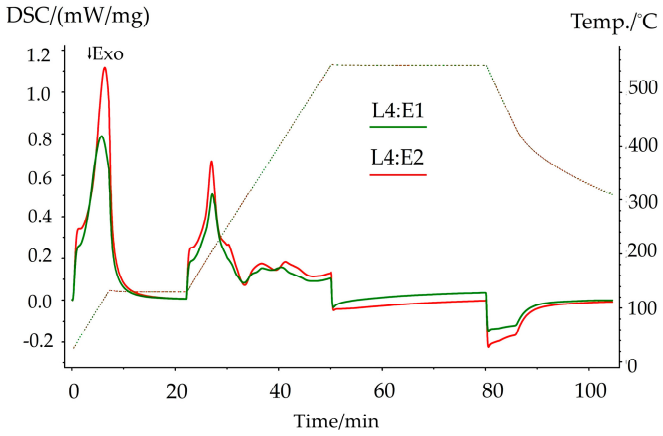

L4: Galvanic sludge 1

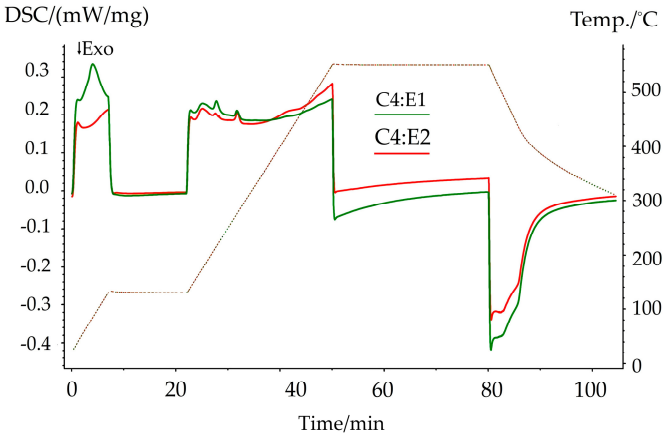

C4: Galvanic catalyst 1

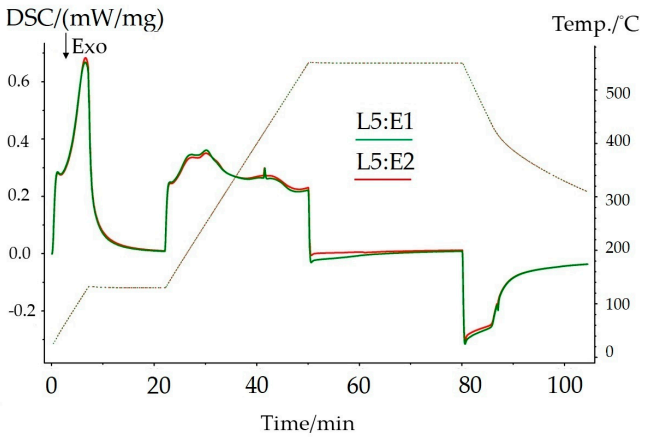

L5: Galvanic sludge 2

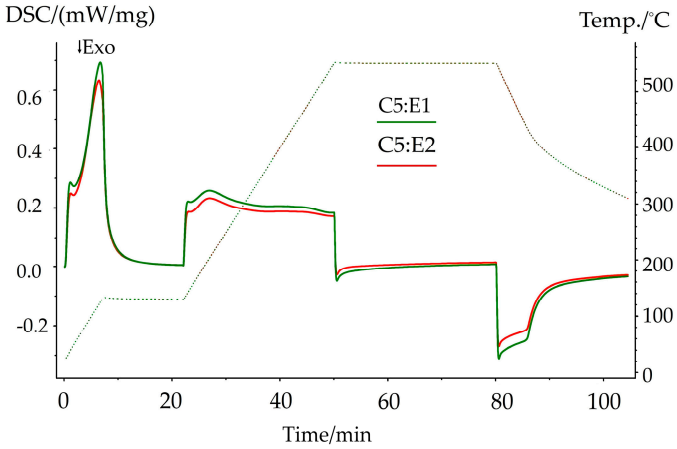

C5: Galvanic catalyst 2

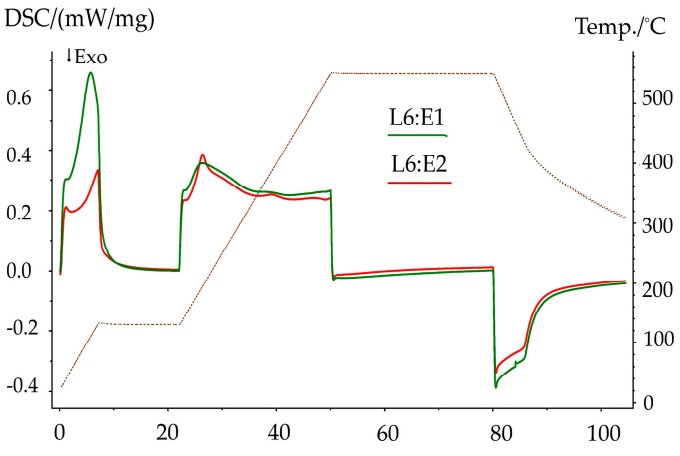

L6: Galvanic sludge 3

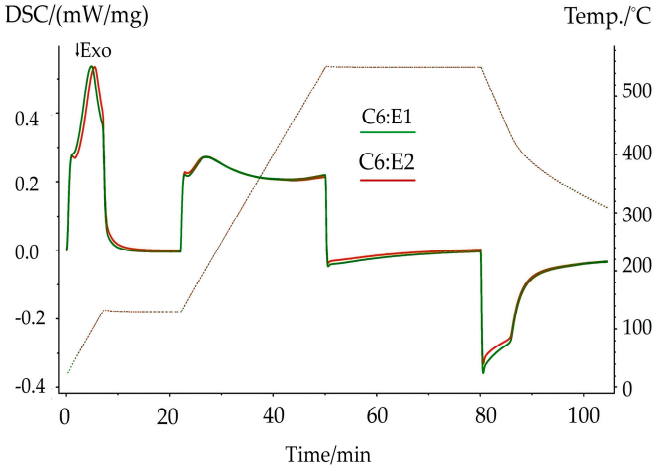

C6: Galvanic catalyst 3

Figure 3. Thermograms of sludge and catalyst from the industry analyzed.

Table 2 shows the temperature and energy of each peak for the DSC thermogram.

Table 2. Energy peaks of sludge and catalysts of the analyzed industries.

Industry		Textile 1		Textile 2		Tannery		Galvanic 1		Galvanic 2		Galvanic 3	
Material	**#**	**T (°C)**	**E (mW/mg)**	**T (°C)**	**E (mW/mg)**	**T (°C)**	**E (mW/mg)**	**T (°C)**	**E (mW/mg)**	**T (°C)**	**E (mW/mg)**	**T (°C)**	**E (mW/mg)**
L	E_1	210 435 483	0.47 0.31 0.33	200 243	0.75 0.7	180 330 515	0.32 1.33 0.32	208 353	0.51 0.15	210 252 422	0.35 0.36 0.29	195	0.36
	E_2	210 425 488	0.52 0.32 0.30	198 243	0.77 0.72	180 330 517	0.27 1.34 0.36	205 352	0.67 0.18	212 250 422	0.34 0.35 0.3	196	0.39
C	E_1	213	0.37	197 259 359	0.35 0.35 0.26	167 332 502	0.59 0.31 0.22	141 176 216 276	0.21 0.23 0.24 0.21	203	0.26	205	0.27
	E_2	210	0.37	200 250 358	0.36 0.35 0.27	167 320 502	0.64 0.33 0.24	142 175 215 277	0.19 0.22 0.2 0.21	205	0.23	205	0.27

For textile industry 1, L1, and C1, we observe endothermic peaks above 200 °C. According to information collected from SiO_2 exposed to DSC, peaks from 200 to 275 °C represent a change in the system's energy content, characteristic of a phase transition from α-SiO_2 to β-SiO_2 [19]. C1 presents fewer peaks and a heat flow of less than 200 °C than L1, indicative of higher thermal stability by the catalyst.

Upon comparing the L1 and L2 sludges with the C1 and C2 catalysts derived from the textile industry, it is suggested that sludges require higher heat fluxes than catalysts. This requirement contributes to enhanced thermal stability in the catalysts.

For the tannery industry, L3 and C3, we distinguished decreasing behavior with differences in shape. The thermogram to C3 presents better visibility of energy peaks, which indicates higher thermal stability than L3.

In the galvanic industry, for L4, decreasing behavior and higher heat fluxes are identified, unlike the catalyst obtained. Hence, the catalyst indicates higher thermal stability with increased heat fluxes from 372 °C. For C4, we observed several energy peaks, possibly due to the diffraction of w-ZnO that increases remarkably with temperature from 167 °C [20] and another endothermic peak belonging to the ε-Fe_2O_3 transition at 220 °C as it approaches the Curie temperature [21].

By comparing thermograms L5 and C5, a decreasing trend is observed in both, indicating a similar behavior of the catalyst with the original sludge, along with lower heat fluxes for the C5 catalyst. In the galvanic industry 2, L5 and C5 present a decreasing behavior, with lower heat fluxes for C5, meaning an endothermic peak from 400 °C; according to the bibliography, this corresponds to the change of iron oxide γ-Fe2O_3 to α-Fe_2O_3 [22]. The analysis of thermograms in galvanic industries shows that catalysts exhibit higher thermal stability compared to sludges, as they require lower heat fluxes.

3.2. Specific Heat

The heat fluxes, given in mW, determine the specific heat for each temperature measurement.

$$Cp = \frac{\Phi_M - \Phi_0}{m * \beta} \quad (2)$$

where:

Cp: specific heat, J/g°C.
Φ_M: heat flux rate of the sample, W.
Φ_0: zero-line heat flux rate, W.
m: mass of the sample, g.
β: heating rate, °C/s.

We segmented the thermogram by peaks due to the large amount of recorded data. When these peaks corresponded to structural changes noted in the literature, we interpolated tracers using splines and obtained polynomials with improved correlation factors. The models corresponded to the third-degree equations (Equation (1)). We selected them according to the compatibility presented by experimental Cp [23], which avoids the value's sensitivity to the rounding of coefficients with polynomials of a higher degree. We selected them based on a bibliography indicating a trend of linear specific heat models for solids and materials at low pressures and in a single phase up to the third degree. Consequently, we developed polynomials for each temperature range, which allow obtaining a value of Cp (J/g°C) as a function of temperature (°C).

The STATGRAPHICS program determined the polynomial regression of one factor. Since the *p*-value for constants in some models is higher than 0.05 (without statistical significance), we calculated a new polynomial with a lower order. Table 3 includes the polynomials for which the model (through ANOVA) and the constants (through *t*-tests) are statistically significant.

Table 3. Regression models of the sludge and catalysts of the analyzed industries.

Sample	Temperature Range (°C)	$Cp = a_1 + a_2T + a_3T^2 + a_4T^3$				
		a_1	a_2	$a_3 \times 10^3$	$a_4 \times 10^6$	R^2
L1	$143 < T \leq 210$	32.3404	−0.5624	3.3343	−6.3837	0.9149
	$210 < T \leq 550$	9.1169	−0.0556	0.1338	−0.1080	0.9342
C1	$143 < T \leq 210$	19.2034	−0.3272	1.9333	−3.6845	0.9962
	$210 < T \leq 550$	4.1590	−0.0189	0.0041	−0.0029	0.9889
L2	$143 < T \leq 235$	21.2360	−0.4175	2.7386	−5.5178	0.9547
	$235 < T \leq 550$	12.1611	−0.0621	0.1173	−0.0077	0.9937
C2	$141 < T \leq 241$	1.9192	−0.0362	0.3165	−0.7272	0.9253
	$241 < T \leq 550$	2.9547	−0.0081	0.0080	0	0.9031
	$185 < T \leq 550$	1.3190	−0.0014	0.0018	0	0.0149
L3	$142 < T \leq 330$	−22.6829	0.3530	−1.6931	2.6756	0.9634
	$330 < T \leq 550$	191.1130	−1.2350	2.6615	−1.8989	0.9292
C3	$142 < T \leq 250$	−52.5590	0.8430	−4.2240	6.8742	0.9136
	$250 < T \leq 550$	−3.1321	0.0410	−0.1160	0.1000	0.8592
L4	$142 < T \leq 205$	12.0252	−0.1451	0.4820	0	0.8570
	$205 < T \leq 550$	15.2246	−0.1121	0.2829	−0.2337	0.8152
C4	$143 < T \leq 375$	−0.2667	0.0179	−0.0740	0.0933	0.7216
	$375 < T \leq 550$	1.6474	−0.0040	0.0058	0	0.7552
L5	$142 < T \leq 227$	13.2004	−0.2174	1.2650	−2.3606	0.9841
	$227 < T \leq 422$	−2.4951	0.0459	−0.1678	0.1889	0.9543
	$422 < T \leq 550$	−35.9233	0.2411	−0.5165	0.3640	0.9338
C5	$142 < T \leq 205$	0.4461	0.0033	0	0	0.5029
	$205 < T \leq 550$	2.5539	−0.0118	0.0284	−0.0233	0.8288
L6	$142 < T \leq 197$	−0.3849	0.0103	0	0	0.8383
	$197 < T \leq 550$	3.3642	−0.0133	0.0256	−0.0164	0.9478
C6	$142 < T \leq 205$	15.8862	−0.2639	1.5407	−2.9325	0.9764
	$205 < T \leq 550$	2.1169	−0.0055	0.0075	−0.0024	0.9945

The fit that is achieved with the Cp models proposed for a temperature interval of 415 to 823 K for each sample of sludge and catalyst from the three industries can be seen in graphs that include the curves corresponding to the polynomials in the different intervals and the thermograms (Figure 4).

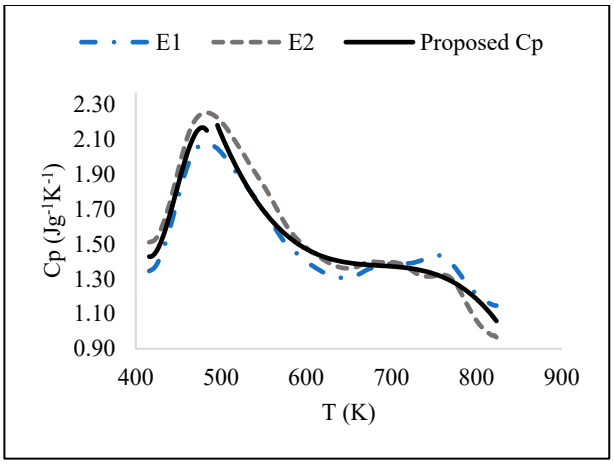

L1: Textile sludge 1

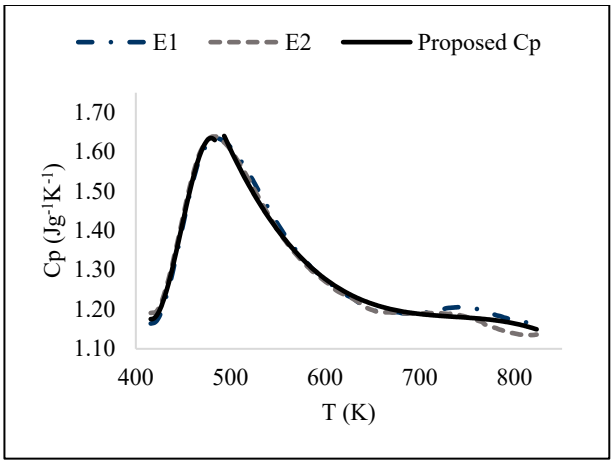

C1: Textile catalyst 1

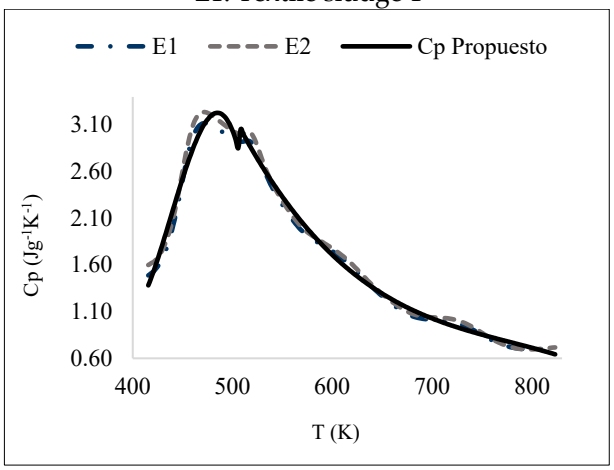

L2: Textile sludge 2

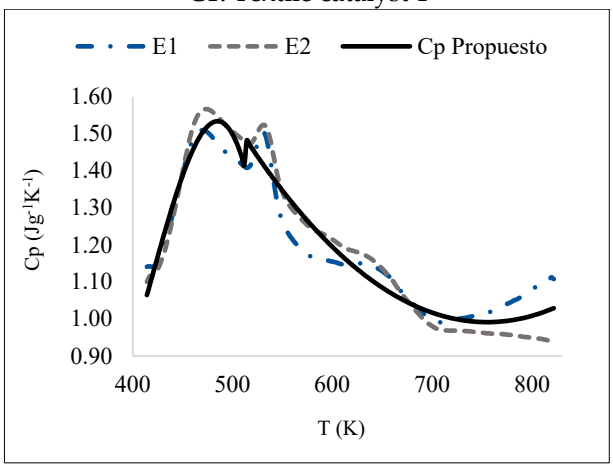

C2: Textile catalyst 2

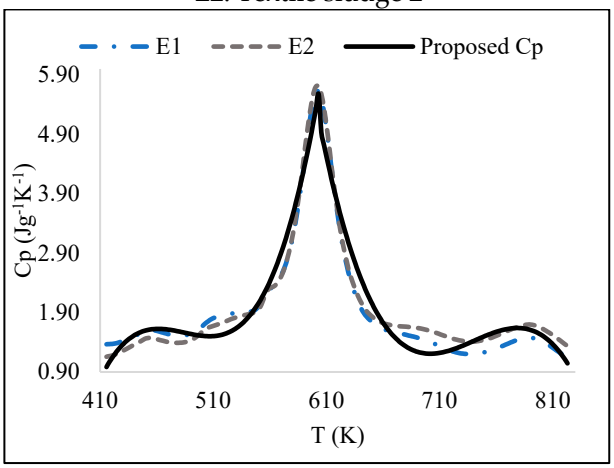

L3: Tannery sludge

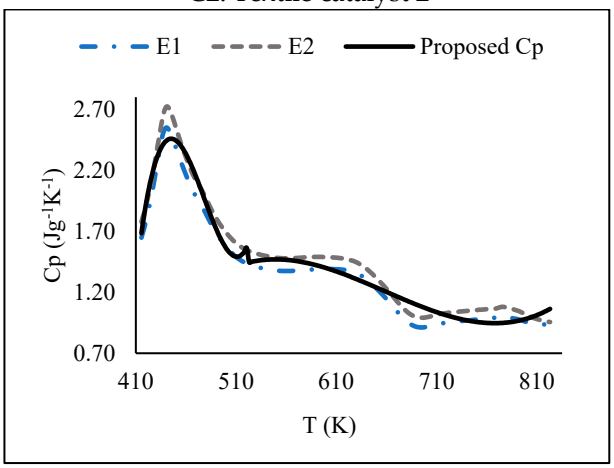

C3: Tannery catalyst

Figure 4. *Cont.*

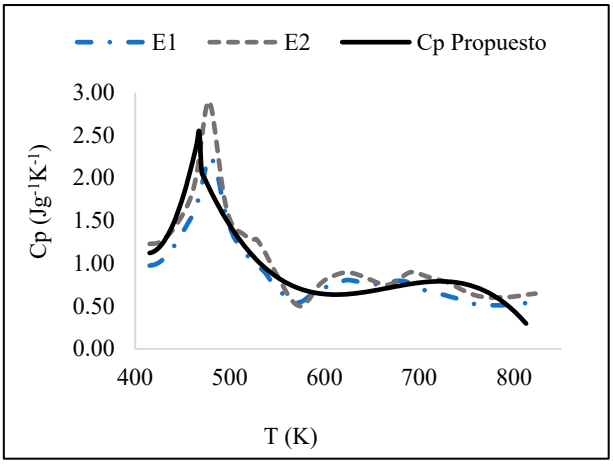

L4: Galvanic sludge 1

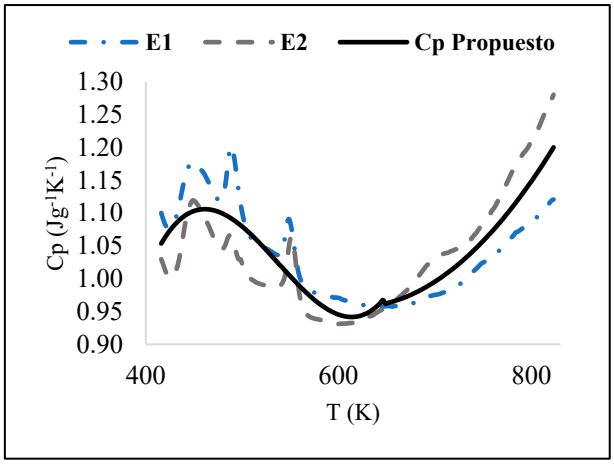

C4: Galvanic catalyst 1

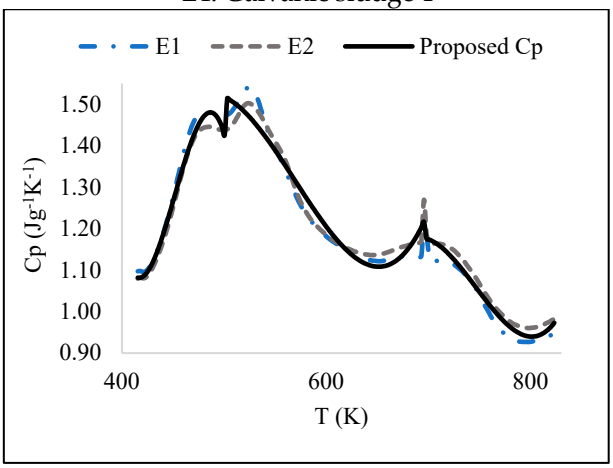

L5: Galvanic sludge 2

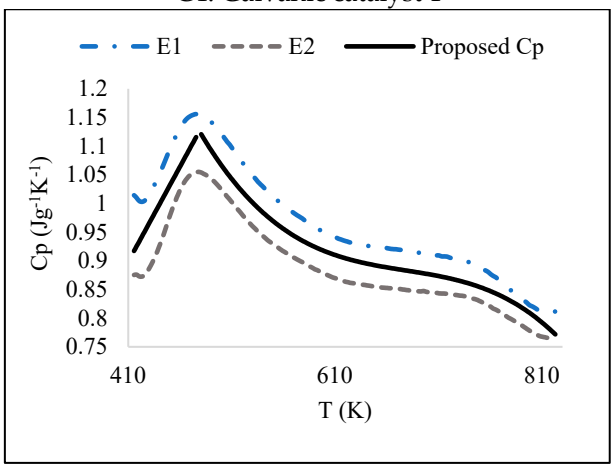

C5: Galvanic catalyst 2

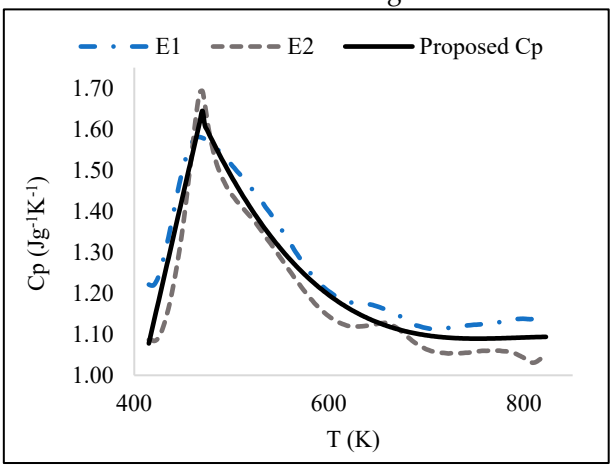

L6: Galvanic sludge 3

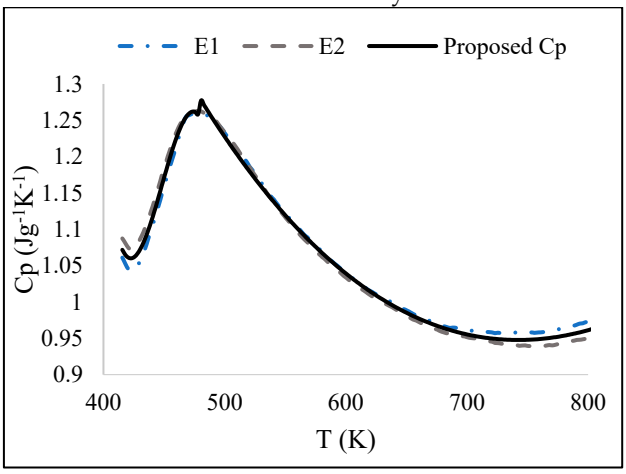

C6: Galvanic catalyst 3

Figure 4. Cp models proposed a 415 to 823 K temperature interval for the analyzed industries.

After correcting the Cp models, the R2 (g.l.) statistics have a low fit with 0.4989 and 0.0149. Huda and Whitney [24] reported an increase in Cp as the material's porosity reduced, so C3 could be influenced by the solid surface's morphology changes when exposed to temperatures higher than the optimum calcination temperatures (400 °C). As the calcination temperatures increase, the number of active sites decreases.

The confidence bands for the value predicted by the model are calculated based on the standard error of the expected value [25]. They allow a comparison of the Cp obtained through the model with bibliographical references, as shown in Table 4.

Table 4. Comparison of Cp C1, C2, C4, C5, and C6 with catalysts and commercial minerals.

Catalyst	Temp. (K)	Other Similar Materials Reported	Cp, This Work (J/g·K)	Cp Reported (J/g·K)	Reference
C1	673.28	Si/Fe/Al	(1.196–1.201)	1.15	[23]
	673.65	Si/Al	(1.196–1.201)	1.252	[26]
	773.15	Si/Fe/Al	(1.171–1.177)	1.18	[23]
	773.65	Si/Al	(1.171–1.177)	1.251	[26]
	800	Fe/Si	(1.160–1.170)	1.08	[27]
	823.11		(1.140–1.160)	1.082	
C2	573.15	Fe/Si	(1.260–1.280)	1.27	[23]
	432.35	Zeolite13X (Si/Al)	(1.160–1.200)	1.17	[28]
	452.15	H-ZSM-5-23 (Si/Al)	(1.340–1.380)	1.39	
	623.15	Fe/Al	(1.130–1.150)	1.12	[29]
	630		(1.120–1.130)	1.1	
C4	583.35	Fe_2TiO_5	(0.948–0.968)	0.956	[30]
	623.15	Fe_3O_4	(0.933–0.954)	0.95	[31]
	673.15		(0.963–0.986)	0.97	
	723.15		(1.010–1.030)	1	
	822.15		(1.180–1.220)	1.1	
C5	573.15	Fe_3O_4	(0.933–0.948)	0.94	[31]
	578.08	Fe_2TiO_5	(0.928–0.943)	0.934	[30]
	640	Fe_2O_3	(0.889–0.902)	0.9	[32]
	643.08	Fe_2O_3	(0.888–0.901)	0.89	[33]
C6	425	FeO	(1.056–1.067)	1.047	[32]
	450	FeO	(1.170–1.180)	1.18	
	673.15	Fe_3O_4	(0.967–0.970)	0.97	[31]

3.3. Enthalpy

Using the specific heat models developed for each sample, the enthalpy change was determined from Equation (3), as shown in Figure 5.

$$\Delta H = H(T) - H(To) = \int_{To}^{T} Cp(T)dT \quad (3)$$

where:

ΔH: enthalpy change (J/g);
Cp: specific heat (J/g·°C).

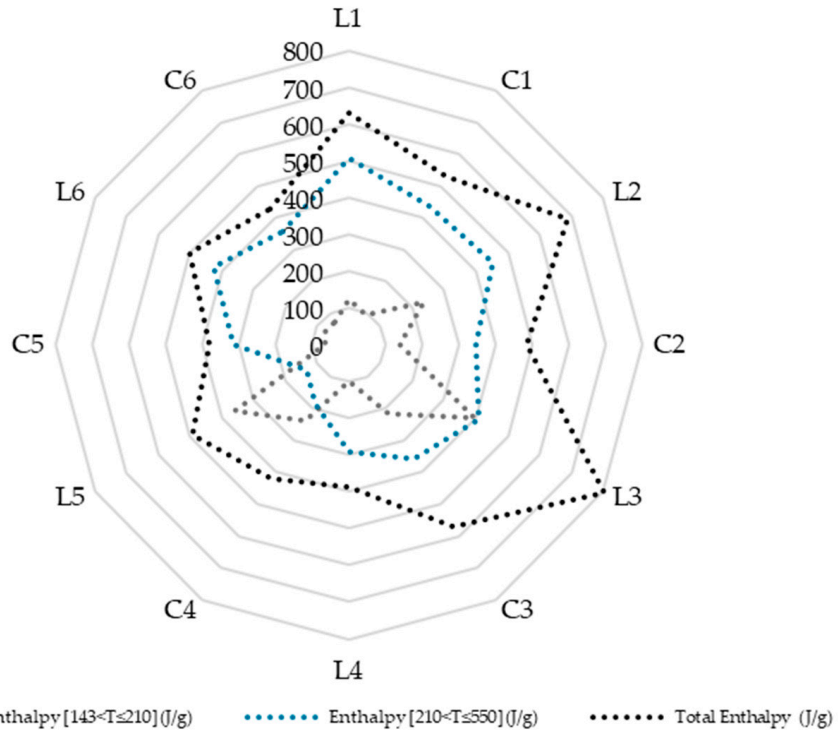

Figure 5. Enthalpy of catalysts and sludge from the textile, tannery, and galvanic industry.

The enthalpy by the catalysts is lower than that determined for the original sludge because most of the catalysts have fewer energy peaks; therefore, there is a lower heat requirement (Figure 5). The C4 strain does not exhibit this behavior. Due to the increase in the number of peaks, the *Cp* variability supposes an endothermic enthalpy 8.77% higher than L4.

The L3 tannery sludge sample reached higher *Cp* values, around 5.90 J/g·°K (Figure 4). It presents a higher total enthalpy value than the other samples (800 J/g), and consequently, the catalyst C3 also corresponds to the highest enthalpy value compared to the other synthesized catalysts (Figure 5). The difference is that this material mainly contains chromium oxides, while industrial sludge is mainly made up of iron oxides. We did not include this in the comparison because we could not find reference materials in the literature to compare it.

C3 is not suitable for achieving a correct energy balance in chemical processes within the tannery industry due to its low model fit. On the other hand, C3 (although no similarity was found) indicates high specific heat values (up to 2.45 J/g·°K at 172 °C), so it could be used in dehydrogenation reactions of alkanes. This reaction requires energy consumption of 2.185 J/g of isobutene produced and the breaking of molecules inside reactions [34].

The lowest enthalpy value corresponds to C6, with a maximum specific heat value of 1.18 J/g·°K.

Additionally, the textile industry samples present similar enthalpy values between sludge and catalysts (L1 = 630.663 J/g, L2 = 686.659 J/g, and C1 = 530.761 J/g, C2 = 486.202 J/g), and they are relatively higher compared to those obtained by other industries.

3.4. Entropy

The entropy change is also calculated using the regression models from Equation (4), as shown in Figure 6.

$$\Delta S = S(T) - S(To) = \int_{To}^{T} \frac{Cp(T)}{T} dT \quad (4)$$

where:

ΔS: entropy change (J/g·K);

Cp: specific heat (J/g·°C).

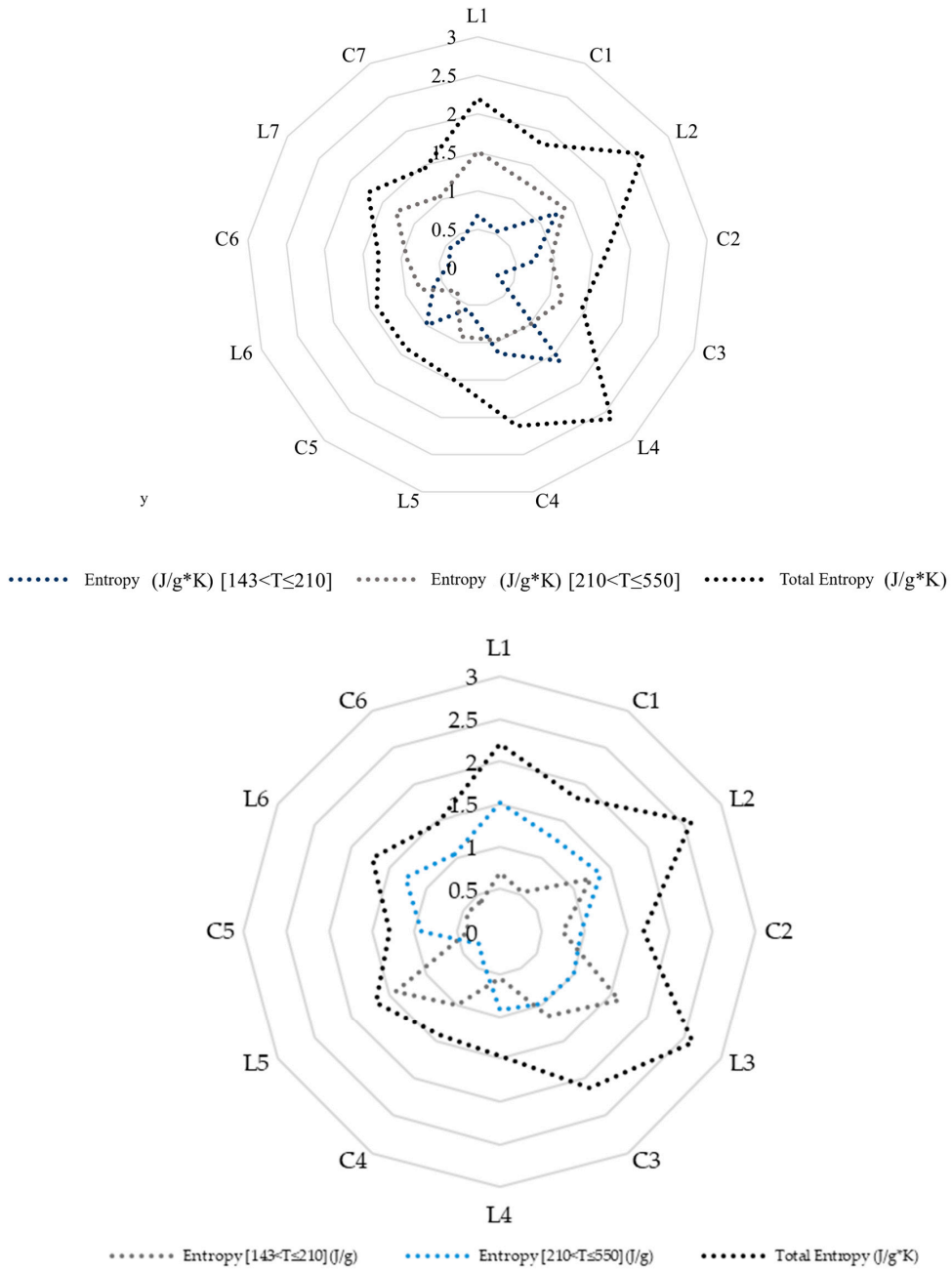

Figure 6. The entropy of catalysts and sludge from the textile, tannery, and galvanic industries.

The entropy of sludge and catalysts from the three industries shows low values not greater than 2.62 J/g·K, since the materials under analysis maintain the characteristics of solids exposed to thermal stability processes (such as calcination to obtain catalyst from sludges), generating limited entropy values. The results show that catalyst entropy values are up to 64% lower than those of their sludge, as thermal stability reduces temperature-induced disorder. This is except for catalyst C5, which presents more significant variability in the model than L5, for which the entropy values are close to those of their original sludge (L5 = 1.467 J/g·°K, C5 = 1.403 J/g·°K).

Similarly, the samples with the highest entropy values are those corresponding to the tannery industry L3 (2.620 J/g·K) and C3 (2.119 J/g·K), in the case of catalysts, since higher entropy variability is expected in materials reaching higher specific heats [35].

4. Conclusions

The specific heat models typically expected for solids exhibit linear behavior because of the materials' thermal stability and homogeneity. However, most calculated specific heat capacity (Cp) models for the three industries demonstrated a good fit with third-degree equations. This discrepancy may be attributed to the heterogeneity of the materials and the structural changes in the components.

Catalyst C3 (tannery) presented high variability between replicates, which caused the prediction model to present low values of R2 (0.4989 and 0.0149). This indicates a low correlation between predictor and response, possibly due to an inverse relationship of Cp with porosity. Since the material was exposed to temperatures higher than the optimal calcination (400 °C), this reduced the number of active sites of the catalyst.

The synthesized catalysts with better specific heat model adjustments belong to the textile industry (C1 and C2). These materials presented a coefficient of determination not less than 0.9031, acceptable for simulating the operating profile and temperature of a reactor, in addition to presenting relatively high enthalpy values (up to 530.761 J/g), which makes them suitable for high-thermal-load industrial processes.

Regarding the catalysts of the galvanic industry, C4 does not indicate thermal stability due to the variations it presents with the increase in temperature, which makes it unsuitable for robust modeling of chemical processes. C5 and C6 indicate similarity with iron oxide components from approximately 300 °C.

Creating catalysts from alternative materials is crucial for enhancing sustainability and minimizing waste. This approach stands in contrast to conventional catalysts, which frequently depend on non-renewable resources. In the following, we present a brief comparison of the advantages and disadvantages of each option.

Catalysts Obtained from Residual Sludge	Commercial Catalysts
Advantages	
Developing catalysts from alternative materials is essential to promote sustainability and reduce waste, in contrast to commercial catalysts that often rely on non-renewable resources. In the following, we present a brief comparison of the advantages and disadvantages of each option. Sustainability and lower environmental impact: It contributes to the circular economy by harnessing waste and reducing the ecological footprint associated with producing conventional catalysts. The cost could be reduced since this material would otherwise require disposal costs. Unique properties: Residual sludge can contain metals and compounds that, depending on their composition, can offer interesting catalytic properties.	Efficiency and performance: designed for specific reactions, offering high efficiency and selectivity. Consistency: provides a uniform and reliable product, an indispensable feature in industrial applications. Easy to use: Handling and application are well documented and standardized, which makes them easy to implement.
Disadvantages	
Variability: Sludge composition variations are significant, which could lead to unfavorable changes in catalyst performance. Efficiency: Catalysts obtained from residual sludge may have a different efficiency or selectivity than commercial ones. Contaminants: May contain impurities or contaminants that negatively affect their performance and the quality of the final product. Reproducibility: Production variability can be a problem in industrial processes to achieve consistent and reproducible results.	Cost: Generally, they are more expensive to produce and acquire. Environmental impact: Production may involve high resource consumption and waste generation. Dependence on raw materials often depends on raw materials that may be scarce or expensive.

This study examines sampled sludges and emphasizes that their characteristics can vary significantly between different companies, even within the same category. This variability, influenced by the raw materials used and the treatment processes employed, is essential for evaluating their effectiveness in specific applications. By understanding these differences, we can optimize treatment and reuse strategies, ultimately reducing the environmental impact of residual sludge management. The potential for producing catalysts from various types of waste presents a valuable opportunity for sustainability and the circular economy. These materials include agro-industrial wastes like biomass and incineration ashes and food industry wastes, particularly seafood. Additionally, we can consider recycling plastics by transforming them into catalysts through depolymerization or pyrolysis processes. Utilizing these wastes will create efficient catalysts and reduce the environmental impact associated with their disposal, promoting a more sustainable approach to industrial waste management.

Author Contributions: G.C.-C., Methodology, Formal analysis, and investigation; J.C., Formal analysis and investigation, Methodology; G.G., Writing—original draft preparation; A.D.-L.-R., Conceptualization, Resources, Writing—review and editing; G.C., Writing—review and editing; C.M.-C., Formal analysis and investigation, Writing—review and editing. All authors have read and agreed to the published version of the manuscript.

Funding: This research was funded by Universidad Central del Ecuador (UCE) through Senior Project No. DI-CONV-2019-005, "CATALYTIC DECOMPOSITION OF METHANE TO OBTAIN H_2 WITH CATALYSTS DERIVED FROM RESIDUAL INDUSTRIAL SLUDGE".

Data Availability Statement: Data will be made available upon request.

Acknowledgments: The publication of this research was possible thanks to a publishing fund granted under the Agreement of Institutional Support 2022-2027 between the Universidad Central del Ecuador (UCE) and the Académie De Recherche Et D'Enseignement Supérieur (ARES) from Belgium. This work is part of the Red Ecuatoriana de Ingeniería de las Reacciones Químicas y Catálisis- RED IRQ-CATEC, recognized by REDU-Ecuador.The authors are grateful to the Research Area for Facultad de Ingenieria Quimica, Universidad Central del Ecuador for their technical support and to all our students who participated in this project.

Conflicts of Interest: The authors declare no conflicts of interest.

References

1. Ley Orgánica de Economía Circular Inclusiva. Ecuador. Available online: https://www.lexis.com.ec/biblioteca/ley-organica-economia-circular-inclusiva (accessed on 17 May 2024).
2. Montero, C.; Castañeda, K.; Oña, Y.; Flores, D.; De La Rosa, A. Catalyst based on sludge derived from wastewater treatment of textile industry. *Chem. Eng. Trans.* **2018**, *70*, 931–936. [CrossRef]
3. Villamarin-Barriga, E.; Canacuán, J.; Londoño-Larrea, P.; Solís, H.; De La Rosa, A.; Saldarriaga, J.F.; Montero, C. Catalytic cracking of heavy crude oil over iron-based catalyst obtained from galvanic industry wastes. *Catalysts* **2020**, *10*, 736. [CrossRef]
4. Kiš, E.; Lomić, G.; Bošković, G.; Marinković-Nedučin, R.; Putanov, P. Controlled re-oxidation of low-pressure methanol synthesis catalyst, followed by means of DSC. *J. Therm. Anal. Calorim.* **1995**, *44*, 1367–1379. [CrossRef]
5. Kök, M.V.; Iscan, A.G. Catalytic Effects of Metallic Additives on The Combustion Properties of Crude Oils by Thermal Analysis Techniques. *J. Therm. Anal. Calorim.* **2001**, *64*, 1311–1318. [CrossRef]
6. Yurchenko, O.; Pernau, H.-F.; Engel, L.; Wöllenstein, J. Differential thermal analysis techniques as a tool for preliminary examination of catalyst for combustion. *Sci. Rep.* **2023**, *13*, 9792. [CrossRef]
7. Tseng, J.; Huang, S.; Duh, Y.; Hsieh, T.; Sun, Y.; Lin, J.; Wu, H.; Kao, C. Thermal analysis and safety information for metal nanopowders by DSC. *Thermochim. Acta* **2013**, *566*, 257–260. [CrossRef]
8. Imran, M.; Raza, M.; Noor, H.; Faraz, S.M.; Raza, A.; Farooq, U.; Khan, M.E.; Ali, S.K.; Bakather, O.Y.; Ali, W.; et al. Insight into mechanism of excellent visible-light photocatalytic activity of CuO/MgO/ZnO nanocomposite for advanced solution of environmental remediation. *Chemosphere* **2024**, *359*, 142224. [CrossRef]
9. Netzer, C.; Løvås, T. Chemical Model for Thermal Treatment of Sewage Sludge. *Chemengineering* **2022**, *6*, 16. [CrossRef]
10. Yang, M.; Baeyens, J.; Li, S.; Li, Z.; Zhang, H. Catalytic methane decomposition on CNT-supported Fe-catalysts. *J. Environ. Manag.* **2024**, *365*, 121592. [CrossRef]

11. De La Rosa Martínez, A.; Ninahualpa, S. Síntesis de Carbono e Hidrógeno a Partir de la Descomposición Catalítica de Metano. Bachelor's Thesis, Universidad Central del Ecuador, Quito, Ecuador, 2022. Available online: http://www.dspace.uce.edu.ec/handle/25000/26305 (accessed on 15 June 2022).
12. Montero, C.; Londono, P.; Alvarado, G. Waste to Chemicals: Obtaining Lactic Acid Through Catalysts Synthesized from Industrial Sludge as an Alternative for Recovering Residual Glycerol—CEDIA. Available online: https://cedia.edu.ec/en/waste-to-chemicals-obtaining-lactic-acid-through-catalysts-synthesized-from-industrial-sludge-as-an-alternative-for-the-recovery-of-residual-glycerol/ (accessed on 12 October 2024).
13. Raza, M.; Farooq, U.; Khan, M.E.; Naseem, K.; Alam, S.; Khan, M.Y.; Ali, W.; Ali, S.K.; Bakather, O.Y.; Al Zoubi, W.; et al. Development of simplistic and stable Co-doped ZnS nanocomposite towards excellent removal of bisphenol A from wastewater and hydrogen production: Evaluation of reaction parameters by response surface methodology. *J. Taiwan Inst. Chem. Eng.* **2024**, *163*, 105654. [CrossRef]
14. De la Rosa Martínez, A.F.; Ponce, D.X.; Bahamontes, L.V. Síntesis de un Material Catalítico a Partir de Lodos Residuales de la Industria de la Curtiembre. Bachelor's Thesis, Universidad Central del Ecuador, Quito, Ecuador, 2017. Available online: http://www.dspace.uce.edu.ec/handle/25000/13208?mode=full (accessed on 15 June 2022).
15. Castro-León, G.; Baquero-Quinteros, E.; Loor, B.G.; Alvear, J.; Montesdeoca, D.E.; De La Rosa, A.; Montero-Calderón, C. Waste to catalyst: Synthesis of catalysts from sewage sludge of the mining, steel, and petroleum industries. *Sustainability* **2020**, *12*, 9849. [CrossRef]
16. Montero Calderón, C.; Moreno Moyano, K.S. Descomposición Catalítica de CH4 Utilizando Catalizadores Derivados de Lodos Residuales de las Industrias: Textil, Galvanoplastia y Curtiembre. Bachelor's Thesis, Universidad Central del Ecuador, Quito, Ecuador, 2020. Available online: http://www.dspace.uce.edu.ec/handle/25000/20703 (accessed on 15 June 2022).
17. *ASTM E1269-01*; Standard Test Method for Determining Specific Heat Capacity by Differential Scanning Calorimetry. ASTM: West Conshohocken, PA, USA, 2017. Available online: https://www.astm.org/e1269-01.html (accessed on 15 June 2022).
18. Brito, J.C. Estudio de las Propiedades Energéticas de Lodos Residuales y Catalizadores de la Industria Textil, Industria de la Curtiembre y Galvanoplastia. Bachelor's Thesis, Universidad Central del Ecuador, Quito, Ecuador, 2021.
19. Leadbetter, A.J.; Wright, A.F. The α—β transition in the cristobalite phases of $SiO_2$and $AlPO_4$I. X-ray studies. *Philos. Mag.* **1976**, *33*, 105–112. [CrossRef]
20. Sokolov, P.S.; Baranov, A.N.; Dobrokhotov, Z.V.; Solozhenko, V.L. Synthesis and thermal stability of cubic ZnO in the salt nanocomposites. *Russ. Chem. Bull.* **2010**, *59*, 325–328. [CrossRef]
21. López-Sánchez, J.; Muñoz-Noval, A.; Castellano, C.; Serrano, A.; del Campo, A.; Cabero, M.; Varela, M.; Abuín, M.; de la Figuera, J.; Marco, J.F.; et al. Origin of the magnetic transition at 100 K inε-Fe_2O_3nanoparticles studied by x-ray absorption fine structure spectroscopy. *J. Phys. Condens. Matter* **2017**, *29*, 485701. [CrossRef]
22. Campos, E.A.; Pinto, D.V.; de Oliveira, J.I.; Mattos, E.D.; Dutra, R.D. Synthesis, characterization and applications of iron oxide nanoparticles—A short review. *J. Aerosp. Technol. Manag.* **2015**, *7*, 267–276. [CrossRef]
23. Waples, D.W.; Waples, J.S. A Review and Evaluation of Specific Heat Capacities of Rocks, Minerals, and Subsurface Fluids. Part 1: Minerals and Nonporous Rocks. *Nat. Resour. Res.* **2004**, *13*, 97–122. [CrossRef]
24. Huda, N.; Whitney, M.A.; Razmpoosh, M.H.; Gerlich, A.P.; Wen, J.Z.; Corbin, S.F. How phase (α and γ) and porosity affect specific heat capacity and thermal conductivity of thermal storage alumina. *J. Am. Ceram. Soc.* **2021**, *104*, 1436–1447. [CrossRef]
25. Abdulagaov, I.M.; Abdulagatova, Z.Z.; Kallaev, S.N.; Omarov, Z.M. Heat-capacity measurements of sandstone at high temperatures. *Geomech. Geophys. Geo-Energy Geo-Resour.* **2019**, *5*, 65–85. [CrossRef]
26. Wen, H.; Lu, J.-H.; Xiao, Y.; Deng, J. Temperature dependence of thermal conductivity, diffusion and specific heat capacity for coal and rocks from coalfield. *Thermochim. Acta* **2015**, *619*, 41–47. [CrossRef]
27. Geiger, C.A.; Dachs, E.; Vielreicher, N.M.; Rossman, G.R. Heat capacity and entropy behavior of andradite: A multi-sample and -methodological investigation. *Eur. J. Miner.* **2018**, *30*, 681–694. [CrossRef]
28. Lu, X.; Wang, Y.; Estel, L.; Kumar, N.; Grénman, H.; Leveneur, S. Evolution of Specific Heat Capacity with Temperature for Typical Supports Used for Heterogeneous Catalysts. *Processes* **2020**, *8*, 911. [CrossRef]
29. Skauge, A.; Fuller, N.; Hepler, L.G. Specific heats of clay minerals: Sodium and calcium kaolinites, sodium and calcium montmorillonites, illite, and attapulgite. *Thermochim. Acta* **1983**, *61*, 139–145. [CrossRef]
30. Enhessari, M.; Razi, M.K.; Etemad, L.; Parviz, A.; Sakhaei, M. Structural, optical and magnetic properties of the Fe_2TiO_5nanopowders. *J. Exp. Nanosci.* **2014**, *9*, 167–176. [CrossRef]
31. Grosu, Y.; Faik, A.; Ortega-Fernández, I.; D'Aguanno, B. Natural Magnetite for thermal energy storage: Excellent thermophysical properties, reversible latent heat transition and controlled thermal conductivity. *Sol. Energy Mater. Sol. Cells* **2017**, *161*, 170–176. [CrossRef]
32. Majzlan, J.; Lang, B.E.; Stevens, R.; Navrotsky, A.; Woodfield, B.F.; Boerio-Goates, J. Thermodynamics of Fe oxides: Part I. Entropy at standard temperature and pressure and heat capacity of goethite (α-FeOOH), lepidocrocite (γ-FeOOH), and maghemite (γ-Fe_2O_3). *Am. Mineral.* **2003**, *88*, 846–854. [CrossRef]
33. Grønvold, F.; Samuelsen, E. Heat capacity and thermodynamic properties of α-Fe2O3 in the region 300–1050 K. antiferromagnetic transition. *J. Phys. Chem. Solids* **1975**, *36*, 249–256. [CrossRef]

34. Velásquez, J.; Rodríguez, G.; Carballo, L. Deshidrogenación oxidativa de isobutano. *Ing. Investig.* **2001**, *48*, 5–11. [CrossRef]
35. Haas, S.; Mosbacher, M.; Senkov, O.N.; Feuerbacher, M.; Freudenberger, J.; Gezgin, S.; Völkl, R.; Glatzel, U. Entropy Determination of Single-Phase High Entropy Alloys with Different Crystal Structures over a Wide Temperature Range. *Entropy* **2018**, *20*, 654. [CrossRef]